

PHOTOPHYSICAL PROPERTIES OF *trans*-2-[4-(DIMETHYLAMINO)STYRYL]-3-ETHYL-1,3-BENZOTHAZOLIUM PERCHLORATE, A NEW STRUCTURAL ANALOG OF THIOFLAVIN T

A. V. Lavysh,^{a*} A. I. Sulatskaya,^b A. A. Lugovskii,^c E. S. Voropay,^c
I. M. Kuznetsova,^{b,d} K. K. Turoverov,^{b,d} and A. A. Maskevich^a

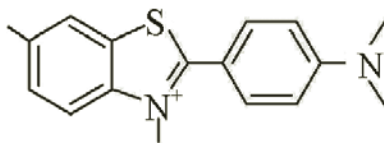
UDC 535.371:577.3

Spectral properties of a newly synthesized thioflavin T (ThT) derivative, trans-2-[4-(dimethylamino)styryl]-3-ethyl-1,3-benzothiazolium perchlorate (DMASEBT) with absorption and fluorescence spectra shifted to longer wavelengths (than ThT), were studied. Quantum-chemical calculations established that DMASEBT is planar in the ground state. The energy minimum of the excited molecule corresponded to a twisted conformation (TICT-state) with a 90° angle between the planar fragments. Charge in the molecule redistributed and a non-fluorescing TICT-state was formed if the fragments rotated. Fluorescence occurred from the non-equilibrium excited state (LE-state). It was shown that limited torsional rotation of the molecular fragments and; therefore, a decreased probability of transitioning into the non-fluorescing TICT-state, were responsible for the significantly increased quantum yield and fluorescence lifetime of DMASEBT upon increasing the solvent viscosity and incorporating it into amyloid fibrils.

Keywords: thioflavin T, *trans*-2-[4-(dimethylamino)styryl]-3-ethyl-1,3-benzothiazolium perchlorate, fluorescence, molecular rotors, amyloid fibrils, intramolecular charge-transfer state.

Introduction. Disruption of protein folding produces incorrectly folded states and stabilizes them through aggregation. This forms ordered insoluble structures known as amyloid fibrils (AF). It is currently thought that the development of diseases such as neurodegenerative Alzheimer's and Parkinson's, prion diseases, etc. is related to the formation and accumulation of AF in various human organs and tissues [1–3]. The study of AF structure has considerable practical value for medicine in the search for ways to prevent their formation and to solve the fundamental problem of protein structural organization and folding.

An effective method for detecting AF *in vivo* and *in vitro* is based on recording fluorescence of the benzothiazole dye thioflavin T (ThT) [4–7]:

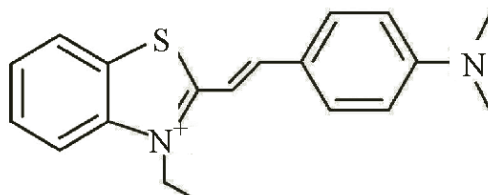


This is due to the fact that this dye in aqueous solution has an extremely low fluorescence quantum yield. Its fluorescence quantum yield increases by almost three orders of magnitude compared with the free dye upon interaction with proteins in the AF state that are enriched in the β -folded structure. Natural ThT or its analogs with absorption and fluorescence spectra that are shifted to longer wavelengths are useful in order to decrease light scattering by fibrils *in vitro* and to diminish absorption and fluorescence of tissues *in vivo*. The creation of such ThT analogs is exceedingly important to testing for AF in living cells and tissues.

*To whom correspondence should be addressed.

^aYanka Kupala State University, 22 Ozheshko Str., Grodno, 230023, Belarus; e-mail: andrewlavysh@mail.ru; ^bInstitute of Cytology, Russian Academy of Sciences, St. Petersburg; e-mail: kkt@incras.ru; ^cBelarusian State University, Minsk; e-mail: voropay@bsu.by; ^dSt. Petersburg State Polytechnical University, Russia; e-mail: imk@incras.ru. Translated from Zhurnal Prikladnoi Spektroskopii, Vol. 81, No. 2, pp. 209–218, March–April, 2014. Original article submitted November 4, 2013.

Herein the spectral properties of newly synthesized ThT derivative *trans*-2-[4-(dimethylamino)styryl]-3-ethyl-1,3-benzothiazolium perchlorate (DMASEBT) are examined:



The absorption and fluorescence spectra of DMASEBT have longer wavelengths than those of ThT. The ability to use the new dye to detect and study AF was demonstrated.

Experimental. The benzothiazole dye DMASEBT was synthesized in the Department of Laser Physics and Spectroscopy, Belarusian State University. Like ThT, DMASEBT is a cation at neutral pH values. A characteristic difference of DMASEBT and ThT is the longer bridge joining the benzene and benzothiazole rings.

Aqueous glycerol solutions (AGS) were prepared by mixing H₂O and 99% glycerol (Sigma-Aldrich, USA) in given ratios. The glycerol content in AGS was determined using the refractive index, which was measured using an Abbe refractometer (LOMO, Russia). AF were prepared by incubating insulin (Sigma, USA) in HOAc (20%) containing NaCl (100 mM) (pH 2.0) at 37°C with constant stirring for 24 h. The solution protein concentration was 2 mg/mL.

Absorption spectra of DMASEBT solutions were recorded on a Specord 200 spectrophotometer (Carl Zeiss, Germany); steady-state solution fluorescence spectra, on an SM2203 spectrofluorimeter (Solar, Belarus). The emission lifetime was measured on a pulsed spectrofluorometer [8] using time-correlated single-photon counting [9]. The fluorescence quantum yield (Φ) of DMASEBT was determined by the comparative method of Williams et al. [10]. The standard for measuring the DMASEBT quantum yield was rhodamine 6G in EtOH, for which $\Phi = 0.98$ [11].

Quantum-chemical calculations of DMASEBT ground and excited states were performed using the PC-GAMESS 7.1.G program (Firefly). The molecular ground state was optimized using a restricted Hartree–Fock (RHF) method in basis set 3-21G. The excited state was calculated using a time-dependent density-functional theory (TDDFT) method with the three-parameter Becke–Lee–Yang–Parr composite exchange-correlated functional (B3LYP).

Results and Discussion. *Quantum-chemical calculations of the DMASEBT structure and ground- and excited-state energies.* The DMASEBT molecule was divided into two fragments. These were I, the benzothiazole ring with an ethyl group (C₂H₅), and II, the benzene ring with the dimethylamino group [N(CH₃)₂]. Two torsion angles that affected most strongly the molecular geometry were selected for optimizing the DMASEBT S_0 ground state structure. These were the angle ψ between the planes formed by atoms 1-2-3 and 2-3-4 and the angle ϕ between the planes formed by atoms 3-4-5 and 4-5-6 (Fig. 1a). Angles $\phi = 0^\circ$ and $\psi = 0^\circ$ corresponded to a planar molecular geometry. The optimization was carried out with fixed angles ϕ and ψ while the other parameters were varied. The ground-state energy E_{S_0} of the conformers as a function of torsion angles (ϕ , ψ) was obtained by varying the angles from 0 to 360° in steps of 10° (Fig. 1b).

Quantum-chemical calculations showed an extremely high energy barrier of $\sim 1.5 \cdot 10^5$ cm⁻¹ for rotation around the C=C bond in the bridge between fragments I and II. Therefore, this rotation was not considered further for the conformational analysis. Rotation of the dimethylamino group relative to the benzene ring was also not considered because such rotation was hindered by a high energy barrier of ~ 2800 cm⁻¹ according to previous quantum-chemical calculations for ThT [12]. An analysis of the potential-energy surface showed that the energy minimum in the ground state corresponded to torsion angles $\phi = 0^\circ$ and $\psi = 0^\circ$.

Thus, the conformational analysis indicated that DMASEBT in the ground state was planar. The energy minimum of the ThT ground state corresponded to an angle of $\phi \approx 37^\circ$ between its two fragments [12]. This was explained by steric interactions of the benzothiazole methyl (CH₃) with the H atoms of the benzene ring. We supposed that the DMASEBT benzothiazole ethyl (C₂H₅) did not interact sterically with the benzene H atoms because of the long ethylene bridge. This made the structure of DMASEBT in the ground state planar.

The energies of the ground (S_0) and Franck–Condon excited (S_1^*) states as functions of ϕ and ψ (Fig. 1c and d) showed that the energy minimum of the excited molecule corresponded to $\phi = 90^\circ$ (for $\psi = 0^\circ$) and $\psi = 90^\circ$ (for $\phi = 0^\circ$). However, the energy minimum of $\sim 10,700$ cm⁻¹ for $\phi = 90^\circ$ was much less than for $\psi = 90^\circ$ ($\sim 17,000$ cm⁻¹). Moreover, a barrier of ~ 1500 cm⁻¹ occurred at $\psi \approx 50^\circ$ for rotation of the benzothiazole ring that increased ψ (Fig. 1c). It could be assumed that rotation of the benzothiazole ring was improbable because of the energy barrier and also because this rotation did not convert the molecule into the lowest energy state.

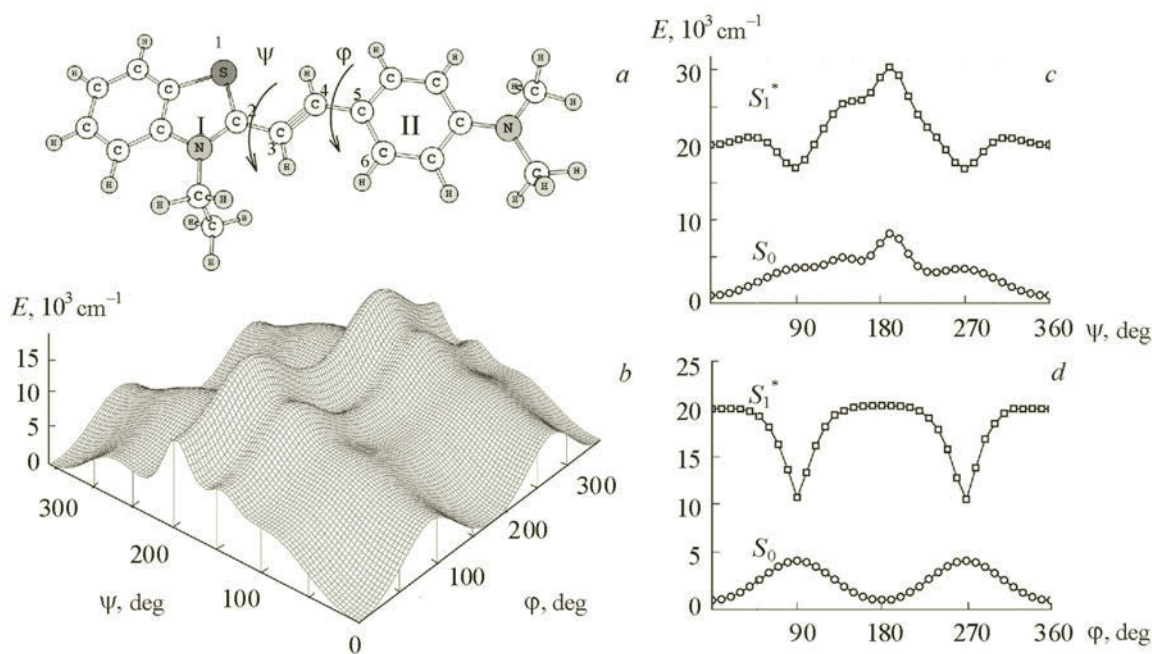


Fig. 1. Molecular structure of DMASEBT with optimized geometry (a), potential energy surface $E_{S_0}(\phi, \psi)$ for DMASEBT ground state (b), and energy of the ground S_0 state and excited Franck-Condon state S_1^* of DMASEBT as functions of angle ψ for $\phi = 0^\circ$ (c) and of ϕ for $\psi = 0^\circ$ (d).

Quantum-chemical calculations indicated that the oscillator strength of electronic transition $S_1^* \rightarrow S_0$ for $\phi = 0^\circ$ was close to unity. However, it decreased as ϕ increased and reached the minimum $f_{S_1^* \rightarrow S_0} \approx 0$ for $\phi = 90^\circ$. The approach of the oscillator strength to zero was a consequence of insignificant overlap of boundary molecular orbitals (MOs), i.e., the lowest unoccupied (LUMO) and highest occupied (HOMO). In fact, Fig. 2 shows that the localization of the boundary MOs changed considerably upon rotation of fragment II. Because the overlap of the HOMO and LUMO was negligibly small for $\phi = 90^\circ$, the probability of a radiative transition became close to zero. This decreased the fluorescence quantum yield. Thus, redistribution of electron density upon rotation of fragment II formed a non-fluorescing twisted state with charge transfer (TICT). A locally excited (LE) state did fluoresce.

Spectral kinetics of DMASEBT fluorescence in various solvents. Figure 3 shows absorption and fluorescence spectra of ThT and DMASEBT in H_2O at pH 5.5. It can be seen that the absorption and fluorescence spectra of DMASEBT were shifted to longer wavelengths by $\approx 100 \text{ nm}$ compared with those of ThT. This shift was due to an expanded π -conjugated system. The position of the DMASEBT absorption spectrum was sensitive to the solvent polarity. Thus, a hypsochromic shift occurred as the polarity increased (Table 1). Analogous spectral changes occurred for ThT solutions [13]. Stabilization of the DMASEBT ground state by polar solvent molecules oriented around it was responsible for the hypsochromic shift. This stabilization was stronger for more polar solvents.

The position of the DMASEBT fluorescence spectrum depended little on the solvent polarity, like for ThT (Table 1). This could be explained as follows. The position of the spectrum was determined mainly by the interaction energy of DMASEBT in the excited state with polar solvent molecules. Torsional rotation of DMASEBT fragments relative to each other prevented the equilibrium state with the solvent from being established. Therefore, the fluorescence was due to transitions from a partially equilibrium excited state into a partially equilibrium ground state. Furthermore, quantum-chemical calculations showed that the oscillator strength and; therefore, the probability of a radiative transition, depended on torsion angle ϕ between the molecular fragments. Rotation of the fragments as a result of torsional relaxation decreased the probability of a radiative transition. The TICT state, for which $\phi = 90^\circ$, was non-fluorescing. Partially relaxed states (for which $\phi < 90^\circ$) had smaller probabilities of a radiative transition and; correspondingly, contributed less to the fluorescence intensity. Finally, a change of solvent polarity that changed the interaction energy of positively charged DMASEBT with polar solvent molecules did not substantially affect the position of the fluorescence spectrum.

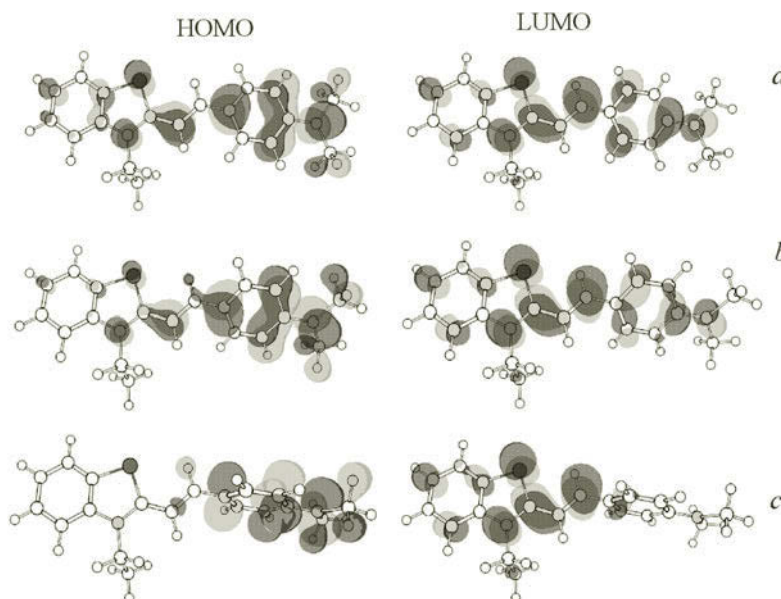


Fig. 2. Boundary molecular orbitals of DMASEBT for $\varphi = 0$ (a), 45° (b), and 90° (c).

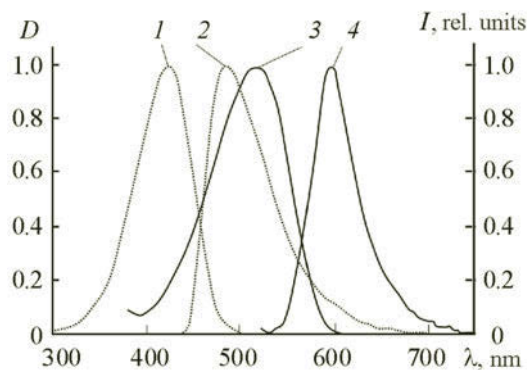


Fig. 3. Normalized absorption (1, 3) and fluorescence (2, 4) spectra of ThT (1, 2) and DMASEBT (3, 4) in H_2O at pH 5.5.

Spectral measurements of DMASEBT in various organic solvents showed a correlation between the Stokes shift of dye fluorescence and the solvent orientational polarizability. Figure 4 shows that the Stokes shift $\Delta\nu_{\text{fl}}$ of DMASEBT fluorescence increased as the orientational polarizability increased. The Stokes shift as a function of orientational polarizability can be described by the Lippert–Mataga equation [14, 15]:

$$hc\Delta\nu_{\text{fl}} = (2\Delta f/a^3)(\Delta\mu)^2 + C_0, \quad (1)$$

where h is Planck's constant; c , the speed of light in a vacuum; a , the radius of the cavity in which the molecule is located (Onsager radius, taken as 4 \AA for DMASEBT) that resulted from geometry optimization of the ground state; $\Delta f = \frac{\epsilon - 1}{2\epsilon + 1} - \frac{n^2 - 1}{2n^2 + 1}$, the solvent orientational polarizability; $\Delta\mu$, the change of dipole moment upon excitation of the molecule; and C_0 , a quantity equal to the Stokes shift for $\Delta f = 0$. The change of DMASEBT dipole moment that was calculated using the angular coefficient function [Eq. (1)] for the transition into the excited state was $\Delta\mu = 4.40 \pm 0.03 \text{ D}$.

Table 1. Spectral Characteristics of DMASEBT in Solvents of Various Polarities

Number	Solvent	Δf	$\lambda_{\text{abs}}^{\text{max}}$, nm	$\lambda_{\text{fl}}^{\text{max}}$, nm	$\Delta\nu_{\text{fl}}$, cm^{-1}	Φ	τ , ns
1	Benzene	0.000	557	601	1314.4	0.017	0.13
2	Toluene	0.013	557	601	1314.4	0.029	0.14
3	1,4-Dioxane	0.021	542	598	1727.8	0.011	0.11
4	CHCl_3	0.149	557	595	1146.6	0.042	0.17
5	Py	0.214	545	606	1847.0	0.017	0.09
6	Glycerol	0.263	544	601	1743.4	0.282	0.91
7	1-Butanol	0.263	538	596	1808.8	0.039	0.11
8	DMSO	0.265	531	610	2438.9	0.017	0.09
9	DMF	0.275	528	607	2464.9	0.005	0.02
10	2-Propanol	0.276	536	594	1821.7	0.008	0.08
11	Acetone	0.284	527	601	2336.4	0.003	0.06
12	EtOH	0.290	534	596	1948.1	0.014	0.05
13	CH_3CN	0.306	524	599	2389.5	0.003	0.01
14	MeOH	0.309	529	597	2153.2	0.007	0.02
15	H_2O	0.320	514	596	2638.9	0.002	0.01

Note. $\lambda_{\text{abs}}^{\text{max}}$ and $\lambda_{\text{fl}}^{\text{max}}$ are wavelength maxima of absorption and fluorescence spectra; Φ , the quantum yield; and τ , the fluorescence lifetime.

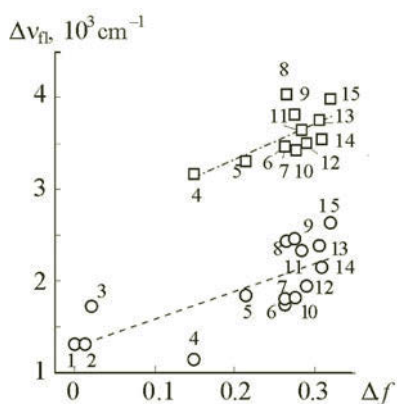


Fig. 4. Fluorescence Stokes shifts of DMASEBT (○) and ThT (□) as functions of solvent orientational polarizability (numbers of points correspond to solvent numbers in Table 1).

Thus, DMASEBT dye in solvents of different polarities experienced the same spectral changes as ThT. This was evident from the similarity of the Stokes shift of their fluorescence as functions of the solvent orientational polarizability (Fig. 4).

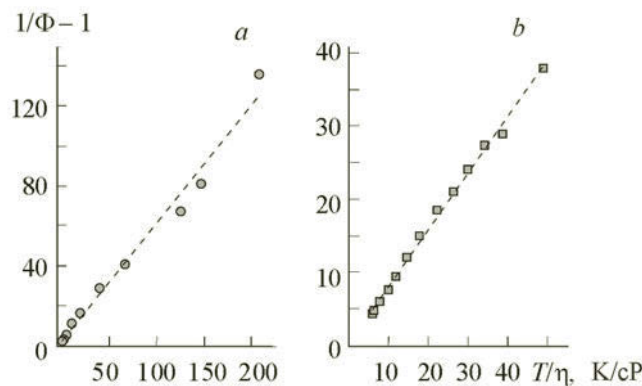


Fig. 5. The quantity $1/\Phi - 1$ as a function of T/η for DMASEBT in aqueous glycerol (a) and in 70% aqueous glycerol at various temperatures (b).

Effect of solvent viscosity on DMASEBT photophysical properties. It was found that the quantum yield and fluorescence lifetime of DMASEBT were strongly dependent on the micro-environment viscosity. The fluorescence intensity of DMASEBT could increase by 2–3 orders of magnitude if the AGS viscosity was increased by cooling or the relative glycerol content in it was increased. Table 1 shows that the DMASEBT fluorescence quantum yield in less viscous solvents was very low although it was an order of magnitude greater than that of ThT [13]. It is important to note that DMASEBT dye was unstable in AGS with a relative glycerol content $\geq 80\%$. The optical density and emission intensity of dye solutions decreased significantly over a rather long time (several days). Increasing the solution temperature accelerated considerably this process. Thus, the optical density was about halved for DMASEBT in 95% AGS at 56°C for 5.5 h. Therefore, AGS with relative glycerol contents $\leq 80\%$ were used to study the DMASEBT quantum yield as a function of temperature and viscosity. The spectral characteristics of such solutions at $\leq 56^\circ\text{C}$ did not change over time.

It was found that the dye emission intensity increased significantly as the glycerol content in the AGS increased. Thus, the DMASEBT fluorescence quantum yield about doubled upon increasing the glycerol content from 15 to 98.5% (Fig. 5a). The DMASEBT fluorescence quantum yield decreased by almost 10 times upon decreasing the viscosity of 70% AGS by heating from 5 to 54°C (Fig. 5b).

The fluorescence quantum yield (Φ) was related to the radiative (k_r) and non-radiative (k_{nr}) rate constants for deactivation of the excited state:

$$\Phi = k_r / (k_r + k_{nr}). \quad (2)$$

An important channel for non-radiative deactivation of aromatic molecules is often intersystem crossing into a triplet state. However, DMASEBT phosphorescence in alcohols or glycerol was not detected at 77 K. Therefore, it was confirmed that intersystem crossing into a triplet state was insignificant and that the main channel for non-radiative deactivation of the DMASEBT excited state was rotation of the benzene ring relative to the benzothiazole that converted the molecule into the non-radiative TICT state. Consider that the rate constant of this non-radiative transition is determined by the rate of rotational diffusion of the benzene ring, i.e., $k_{nr} \sim k_{rot}$. We use the Debye–Stokes–Einstein equation to determine the rotational diffusion rate [16]:

$$k_{rot} = (3k_B/4\pi\rho^3)(T/\eta), \quad (3)$$

where k_B is Boltzmann's constant; ρ , the effective hydrodynamic radius of the rotated molecular fragment; η , the solvent viscosity; and T , the solvent temperature.

We have from Eqs. (2) and (3), the function

$$1/\Phi - 1 = (3k_B/4\pi\rho^3 k_r)(T/\eta), \quad (4)$$

which was also characteristic of ThT in glycerol and AGS [17]. Linear functions were also obtained for DMASEBT in AGS and 70% AGS at various temperatures (Fig. 5).

Because torsional rotation of the molecular fragments was impossible at infinitely large viscosity, the fluorescence quantum yield should be equal to unity according to Eq. (2), i.e., $(1/\Phi - 1)_{T/\eta \rightarrow 0} \rightarrow 0$. However, the functions shown in Fig. 5 did not pass through the origin for $T/\eta \rightarrow 0$ but intersected the ordinate at a certain point above zero. Hence, the fluorescence quantum yield was less than unity at infinitely large viscosity. This discrepancy indicated that the non-radiative transition of the molecule into the ground state that was related to torsional rotation of its fragments was not the only deactivation pathway. It is noteworthy that the DMASEBT fluorescence lifetime increased from 0.05 to 0.93 ns in AGS as the glycerol content increased from 15 to 98.5%. Thus, the DMASEBT quantum yield and fluorescence lifetime depended to a large extent on the solvent viscosity. This was characteristic of molecular rotors [18–20], one of which was ThT [21].

The viscosity of many solvents as a function of temperature can be written

$$\eta^{-1} = \eta_0^{-1} \exp(-\Delta E_\eta/k_B T), \quad (5)$$

where ΔE_η is the activation energy of solvent viscous flow [22]. Literature data [22] were used to construct a plot of the natural logarithm of the viscosity of 70% AGS vs. inverse temperature, the slope of which enabled the activation energy of solvent viscous flow to be determined as $\Delta E_\eta = 2552 \pm 107 \text{ cm}^{-1}$.

We obtain from Eq. (4) the expression

$$(1/\Phi - 1)(1/T) \sim 1/\eta,$$

and find by combining it with Eq. (5)

$$(1/\Phi - 1)(1/T) \sim \exp(-\Delta E_\Phi/k_B T),$$

where ΔE_Φ is the activation energy of torsional rotation; for DMASEBT in 70% AGS, $\Delta E_\Phi = 1442 \pm 89 \text{ cm}^{-1}$. A comparison of ΔE_η and ΔE_Φ indicated that rotation of DMASEBT fragments in the excited state was not related to overcoming the internal activation barrier but was due exclusively to the solvent viscosity.

The results confirmed the conclusions that were drawn based on the quantum-chemical calculations that the DMASEBT excited state was deactivated by torsional relaxation combined with rapid rotation of the aromatic rings relative to each other. Such a rotation, which formed the twisted non-fluorescing TICT state, was a quenching process. If the viscosity of the medium in which the dye was located was high, then rotation of the molecular fragments would be hindered. This would decrease the transition rate constants into the non-radiative TICT state and; thereby, increase the fluorescence quantum yield. In fact, the experimental results showed that DMASEBT fluorescence in slightly polar solvents typically had a low quantum yield. The DMASEBT quantum yield increased significantly in viscous solvents.

DMASEBT solutions, like those of ThT, were characterized by high degrees of polarization through the whole emission spectrum. The fluorescence polarization was close to 0.5 in both aqueous solution and 99% glycerol, i.e., increasing the solution viscosity by three orders of magnitude increased the quantum yield by two orders of magnitude but had practically no effect on the emission anisotropy. Let us identify the two principal reasons for the high degree of fluorescence polarization. First, the characteristic time for Brownian rotation of DMASEBT as a whole that depolarized the fluorescence was significantly longer than the time for torsional rotation, which was a quenching process. The high degree of polarization and the weak dependence of the emission spectrum maximum confirmed that the emission occurred from a non-equilibrium locally excited LE state. The relaxed TICT state that resulted from rotation of the molecular fragments by 90° was non-fluorescing. Second, quantum-chemical calculations indicated that the radiative transition dipole moment for DMASEBT and ThT was directed along the long axis. Its orientation was independent of the angle between the molecular fragments.

Spectral properties of DMASEBT in the presence of proteins and AF. Because it was found that torsional rotation of DMASEBT molecular fragments was hindered in viscous solvents, it was natural to assume that torsional rotation was also hindered in rigid media, e.g., upon incorporation into macromolecules. We measured spectra of aqueous solutions of DMASEBT in the presence of bovine serum albumin (BSA), human serum albumin (HSA), and AF prepared from insulin. The measurements (Fig. 6, inset) showed that the position of the fluorescence spectrum did not change and the dye emission intensity increased insignificantly for albumin concentrations up to $84 \mu\text{g/mL}$. Conversely, the DMASEBT fluorescence intensity increased considerably in the presence of AF (Fig. 6). This could be explained by the fact that dye molecules were incorporated into the AF structure upon interaction of DMASEBT with AF. As a result, the rigidity of their micro-environment increased. This hindered torsional rotation of DMASEBT fragments and decreased the transition rate constants into the non-fluorescing TICT state. The final result was an increased dye fluorescence quantum yield.

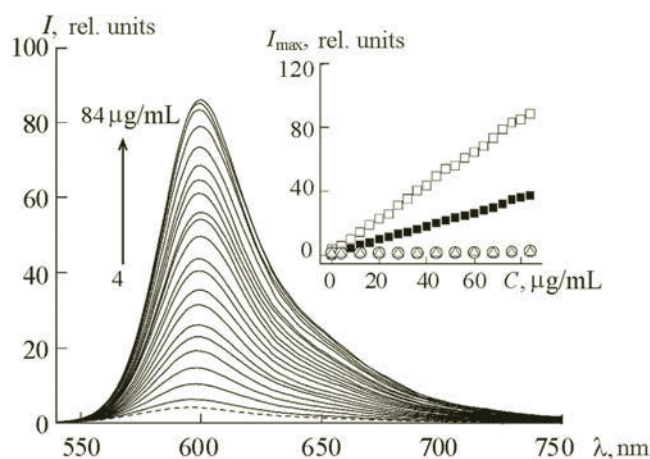


Fig. 6. DMASEBT fluorescence spectra in the presence of various concentrations of insulin amyloid fibrils; dashed line, fluorescence spectrum of free dye ($\lambda_{ex} = 480$ nm); in the inset, fluorescence intensity of DMASEBT + AF (\square), DMASEBT + HSA (\circ), DMASEBT + BSA (Δ), and ThT + AF (\blacksquare) at the spectrum maximum I_{max} as functions of AF, HSA, and BSA concentration.

The optical density of DMASEBT absorption increased slightly and its spectral position did not change if AF were added. Such insignificant changes of the absorption spectrum could be explained by the fact that the fraction of probe molecules incorporated into AF was small at the used protein concentrations. Figure 6 (inset) also shows ThT fluorescence intensity as a function of AF concentration. It can be seen that DMASEBT fluorescence intensity was ~ 1.5 times greater than that of ThT for identical AF concentrations. The optical densities at the excitation wavelengths of solutions of both dyes without AF were identical at 0.06.

Although ThT is also considered to be a specific probe for AF, the presence of BSA or HSA at concentrations of 1.5 mg/mL increased the probe emission intensity by 10 and 4 times [24, 25]. The DMASEBT fluorescence intensity increased by 4 and 2.5 times at high BSA and HSA concentrations (1.5 mg/mL). Thus, DMASEBT was a more specific probe for AF than ThT. DMASEBT was convenient for use in biophysical research, in particular for studying AF and their formation processes in solution and living cells and tissues, because its absorption and fluorescence spectra were shifted by ≈ 100 nm to longer wavelengths compared with those of ThT.

Conclusions. Quantum-chemical calculations and spectral studies found that the new synthesized dye DMASEBT, which was a ThT derivative, had properties characteristic of molecular rotors. The molecule in the ground state was planar. Fluorescence occurred from a non-equilibrium locally excited state (LE state). The molecule energy minimum in the excited state corresponded to a twisted conformation (TICT state) in which the angle between the fragment planes was 90° . Charge in the molecule redistributed upon rotation of the fragments and formed a non-fluorescing TICT state. It was found that the micro-environment viscosity affected the torsional rotation rate of the molecular fragments and; therefore, the transition probability into the non-fluorescing TICT state. This was reflected in the significant increase of the DMASEBT fluorescence quantum yield upon increasing the solvent viscosity. The DMASEBT fluorescence intensity also increased in the presence of AF based on insulin. This could be explained by incorporation of dye molecules into the fibrils. The rigidity of the micro-environment prevents rotation of the molecular fragments, thereby hindering the transition into the TICT state. The position of DMASEBT absorption and fluorescence spectra at long wavelengths made this dye a convenient probe for detecting AF and studying their formation processes.

Acknowledgments. We are deeply grateful to Dr. Phys.-Mat. Sci. V. A. Kuz'mitskii for useful discussions of the quantum-chemical calculations. The work was supported financially by the Belarusian Republic Foundation for Basic Research (Contract No. F12R-198), the Russian Foundation for Basic Research (Contracts Nos. 12-04-90022-Bel_a, 13-04-02068, and 12-04-01651), the RF Ministry of Education and Science (Agreement No. 14.132.21.1311), the RF President Grant Committee (Stipend SP-776.2012.4), and the RAS Presidium Program Molecular and Cellular Biology.

REFERENCES

1. J. D. Harper, C. M. Lieber, and P. T. Lansbury, Jr., *Chem. Biol.*, **4**, 951–959 (1997).
2. J. W. Kelly, *Structure*, **5**, 595–600 (1997).
3. R. W. Carrell and B. Gooptu, *Curr. Opin. Struct. Biol.*, **8**, 799–809 (1998).
4. H. Naiki, K. Higuchi, M. Hosokawa, and T. Takeda, *Anal. Biochem.*, **177**, 244–249 (1989).
5. H. LeVine III, *Methods Enzymol.*, **309**, 274–284 (1999).
6. H. LeVine, *Protein Sci.*, **2**, 404–410 (1999).
7. E. S. Voropay, M. P. Samtsov, K. N. Kaplevskii, A. A. Maskevich, V. I. Stepuro, O. I. Povarova, I. M. Kuznetsova, K. K. Turoverov, A. L. Fink, and V. N. Uverskii, *Zh. Prikl. Spektrosk.*, **70**, No. 6, 767–773 (2003).
8. A. A. Maskevich, V. I. Stepuro, S. A. Kurguzenkov, and A. V. Lavysh, *Vestn. Grodn. Gos. Univ.*, **159**, No. 3, 107–119 (2013).
9. D. V. O'Connor and D. Phillips, *Time-Correlated Single Photon Counting*, Academic Press, New York (1984), pp. 37–54.
10. A. T. R. Williams, S. A. Winfeld, and J. N. Miller, *Analyst*, **108**, 1067–1071 (1983).
11. J. Hung, J. Castillo, and A. Marciano Olaizola, *J. Lumin.*, **101**, 263–268 (2003).
12. V. I. Stsiapura, A. A. Maskevich, V. A. Kuzmitsky, K. K. Turoverov, and I. M. Kuznetsova, *J. Phys. Chem. A*, **111**, 4829–4835 (2007).
13. A. A. Maskevich, V. I. Stsiapura, V. A. Kuzmitsky, I. M. Kuznetsova, O. I. Povarova, V. N. Uversky, and K. K. Turoverov, *J. Proteome Res.*, **6**, 1392–1401 (2007).
14. E. Lippert, *Z. Elektrochem.*, **61**, 962–975 (1957).
15. N. Mataga, Y. Kaifu, and M. Koizumi, *Bull. Chem. Soc. Jpn.*, **29**, 465–470 (1956).
16. A. Einstein, *Ann. Phys.*, **19**, 371–381 (1906).
17. A. I. Sulatskaya, A. A. Maskevich, I. M. Kuznetsova, V. N. Uversky, and K. K. Turoverov, *PLoS One*, **5**, No. 10, e15385 (2010).
18. N. Koumura, E. M. Geertsema, A. Meetsma, and B. L. Feringa, *J. Am. Chem. Soc.*, **122**, No. 48, 12005–12006 (2000).
19. N. Koumura, R. W. O. Zijlstra, R. A. Van Delden, N. Harada, and B. L. Feringa, *Nature*, **401**, No. 6749, 152–155 (1999).
20. D. A. Leigh, J. K. Wong, F. Dehez, and F. Zerbetto, *Nature*, **424**, No. 6945, 174–179 (2003).
21. V. I. Stsiapura, A. A. Maskevich, V. A. Kuzmitsky, V. N. Uversky, I. M. Kuznetsova, and K. K. Turoverov, *J. Phys. Chem. B*, **112**, No. 49, 15893–15902 (2008).
22. R. O. Loutfy and B. A. Arnold, *J. Phys. Chem.*, **86**, 4205–4211 (1981).
23. J. B. Segur, C. S. Miner, and N. N. Dalton, *Physical Properties of Glycerol and Its Solutions in Glycerol*, Reinhold Publ. Corp., New York (1953), pp. 238–334.
24. A. A. Maskevich, S. A. Kurguzenkov, and A. V. Lavysh, *Vestn. Grodn. Gos. Univ.*, **151**, No. 2, 75–85 (2013).
25. P. Sen, S. Fatima, B. Ahmad, and R. H. Khan, *Spectrochim. Acta, Part A*, **74**, 94–99 (2009).